WAXD meridional amorphous scattering of α-form nylon-6 fibres

Po-Da Hong* and Keizo Miyasaka
Department of Organic and Polymeric Materials, Tokyo Institute of Technology, Meguro-ku, Tokyo 152, Japan
(Received 24 June 1991; revised 5 August 1991; accepted 4 September 1991)

A new method of evaluation for the meridional amorphous X-ray scattering of nylon-6 fibres is proposed. The facts (1) that the observed (040) profile is broader than those from other (0*k*0)s and (2) that the value of the crystallite orientation function evaluated from the (040) peak is smaller than those from other (0*k*0)s are considered to be due to the amorphous scattering overlapping on the crystal (040) diffraction. Under these circumstances, the profile of the meridional amorphous scattering overlapping on the crystal (040) profile was evaluated by a new method. This method is based on the condition that the observed (020), (060), (0140) profiles are hardly affected by the amorphous scattering because such scattering has no structure in the regions of their diffraction angles. The results show that the change of observed (040) profile with extension of fibres is not only due to the increase of crystallite size, as suggested by Kaji (*Makromol. Chem.* 1974, **175**, 311)[1], but also to the concentration of the amorphous scattering caused by orientation.

(Keywords: X-ray diffraction; amorphous scattering; nylon-6 fibres; meridional diffraction; extension)

INTRODUCTION

Semicrystalline polymers usually consist of crystalline and amorphous phases, so X-ray diffraction from them is contributed to by both phases. Since the separation of each contribution of X-ray diffraction intensity has long been an important problem, many separation methods have been proposed in studies of crystallinity and intensity profiles[2–5]. In many cases, such as polyethylene and nylon-6, the amorphous X-ray scattering in a sample is assumed to be the same as the scattering intensity profiles observed for the molten state or for quenched samples. These methods may be reasonable for samples without any molecular orientation. The change must be small in isotropic samples, even if the profile of amorphous scattering might depend on the sample history.

Recently, Murthy and Minor[6] used a profile-fitting technique in evaluating amorphous scatterings in X-ray diffraction of semicrystalline polymers and reported that nylon-6 has a maximum amorphous scattering at *ca.* $2\theta = 21°$ at room temperature. Heuvel *et al.*[7] and Gurato *et al.*[8] also employed some mathematical models to determine the shape and position of the amorphous scattering of nylon-6. All of these studies were for the isotropic state of the amorphous phase. The structure of the amorphous phase is not completely random and is more or less ordered in drawn and oriented samples. Generally speaking, difficultly still remains in the estimation of a reliable amorphous scattering profile in oriented semicrystalline samples. It is well known that orientation induced by unixaxial drawing sometimes produces very sharp scattering from amorphous polymers such as polystyrene (PS)[9] and poly(methyl methacrylate) (PMMA)[10].

In this study, an attempt is made to separate the crystalline and amorphous scatterings on the meridian of an α-form nylon-6 fibre by using some basic theories of X-ray diffraction. Nylon-6 has seven serial meridional orders of (0*k*0) diffractions and the amorphous scattering peak seems to appear at the scattering angle where the (040) diffraction appears[6–8]. Our basic conceptions of the method proposed here are: (1) the breadths of diffraction profiles must be the same for all the (0*k*0) diffractions after being corrected for the lattice disorder factors; and (2) the azimuthal intensity distribution for all the (0*k*0) diffractions must be the same, for it depends only on the crystallite orientation. If there are any significant deviations from these expectations, they are assumed to have resulted from the error in the estimation of the crystalline (0*k*0) profile, which implies inaccuracy in estimating amorphous scattering. As will be seen later, significant deviations are seen in the results from the (040) diffraction, so that is where our interest is concentrated. The important and favourable situation in this case is (1) that the profile of the (0140) diffraction is reasonably assumed to be unaffected by amorphous scattering because it has no structure at such a large diffraction angle, and (2) that the amorphous scattering peak of nylon-6 seems to have only one peak near the (040) peak.

The change in the meridional profiles of the amorphous scattering by extension of the fibre was also investigated. The results showed that the sharpening of the apparent (040) diffraction profile is not only due to the increase of crystallite size, as first reported by Kaji[1], but also to the remarkable concentration of amorphous scattering.

EXPERIMENTAL

Samples

A highly oriented α-form nylon-6 tire cord (untwisted) was used as a sample, which was kindly supplied by

* Present address: Department of Textile and Polymer Engineering, National Taiwan Institute of Technology, Taipei 10672, Taiwan

0032-3861/92/183828-05

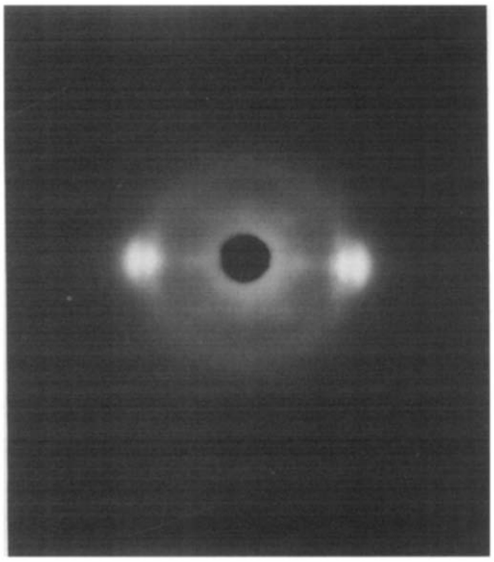

Figure 1 WAXD photograph of the original (0%) nylon-6 fibre

Teijin Co. Ltd, Japan. In order to get a more complete α-form crystalline sample, the fibres were annealed for 1 h at 180°C under steady state conditions. They were then aligned parallel in order to make a plate-shaped specimen about 1 mm in thickness. The specimen was stretched by 12% and kept in a Tensilon for 6 h before being fixed to a stainless steel X-ray sample holder, without relaxation of the extension.

Figure 1 shows a wide-angle X-ray diffraction (WAXD) photograph of the original (0%) sample, which indicates a complete fibre pattern from α-form nylon-6 crystallites.

Measurements of X-ray diffraction

WAXD intensity was measured with graphite-monochromated CuKα radiation (wavelength, 1.54 Å (1 Å = 10^{-10} m)), generated at 50 kV and 180 mA in a Rigaku Rota Flex RU200 diffractometer, by using a scintillation counter with a pulse-height analyser. WAXD meridional intensity profiles obtained at a scan speed of 0.25° min^{-1} were corrected for air scattering and standardized by quantity of sample. The instrumental broadening was corrected by using silicon powder as a standard material. The crystallite orientation function, f_c, was evaluated by the azimuthal scanning of the (0k0) diffraction at a scan speed of 2° min^{-1}. The unit cell of α-form nylon-6[11] is monoclinic with lattice constants $a = 9.56$ Å, $b = 17.24$ Å (chain axis), $c = 8.01$ Å and $\beta = 67.5°$.

RESULTS AND DISCUSSION

Figure 2 shows the observed WAXD meridional intensity profiles for 0% and 12% stretched samples. *Figure 2* indicates that the (040) diffraction is much broader than other (0k0)s, implying that the observed (040) profile may be superimposed by a strong amorphous scattering peak. Generally, the diffraction profiles broaden with lattice distortion, according to paracrystalline[12] or microstrain[13] modes. The (020), (040), (060) and (0140) profiles were used to analyse the breadth due to the lattice distortion in the chain direction, according to both the microstrain and paracrystalline modes.

If the profiles were assumed to be Gaussian, then the observed breadth, ΔS, is given by

$$\Delta S^2 = \Delta S_c^2 + \Delta S_d^2 \quad (1)$$

where ΔS_c^2 and ΔS_d^2 are contributions from the size and disorder, and the breadth is given by

$$\Delta S = 2\Delta\theta[(\cos\theta)/\lambda] \quad (2)$$

Here $S = (2\sin\theta)/\lambda$, $2\Delta\theta$ is the integral breadth of the diffraction, θ is the Bragg angle and λ is the wavelength of X-rays. ΔS is given to a microstrain mode

$$\Delta S^2 = (1/L_{0k0})^2 + (4\pi g^2/d_{0k0}^2)k^2 \quad (3)$$

and to a paracrystalline mode

$$\Delta S^2 = (1/L_{0k0})^2 + (\pi^4 g^4/d_{0k0}^2)k^4 \quad (4)$$

where L_{0k0} is the crystallite thickness in the chain direction (crystallite size in the direction normal to the (0k0) plane), d_{0k0} is the (0k0) spacing, g is the relative distance fluctuation of d_{0k0} and k is the order of the reflection.

Figures 3a and *b* show the ΔS^2 *versus* k^2 and ΔS^2 *versus* k^4 plots, where ΔS was evaluated from the observed diffraction profiles by using the amorphous background shown by broken lines in *Figure 2*. It may be reasonable to assume that these broken lines work satisfactorily well except for the (040) diffraction. This may be due to the fact that the profiles of the (0k0) peaks, except for (040), are hardly affected by the amorphous scattering so, in other words, the separation of the crystalline intensity from the amorphous background was performed reasonably well by the broken line. A linear relation, except for (040), is better satisfied for the ΔS^2 *versus* k^2 plot in *Figure 3a* than for the ΔS^2 *versus* k^4 plot in *Figure 3b*: in this case, the microstrain mode better describes the lattice distortion in the chain direction of α-form nylon-6 crystallites than the paracrystalline mode. It should be noted that the same results were reported by Murthy[14] for γ-form nylon-6 fibres, while Kaji[1] suggested that the lattice distortion of the same materials obeys the paracrystalline mode. The values of g and the crystallite size, L, estimated from *Figure 3a* by using equation (3), are 0.30%, 0.36% and 73 Å, 83 Å for the (010) diffraction of the 0% and 12% stretched samples, respectively.

However, the breadth of the observed (040) profile

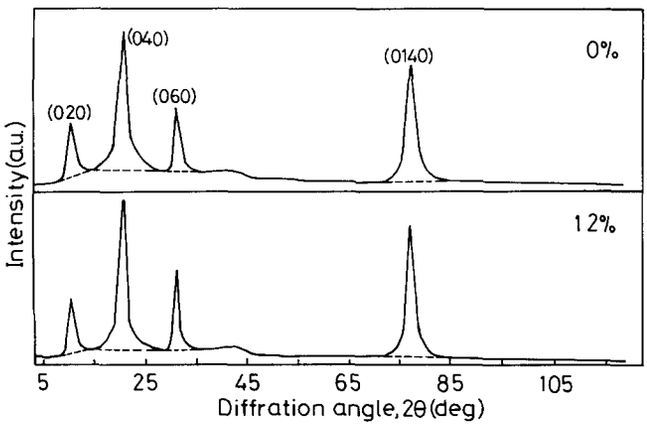

Figure 2 Meridional intensity profiles of the nylon-6 fibre: the broken lines represent the provisional baseline of amorphous scattering for evaluating the observed breadth, ΔS

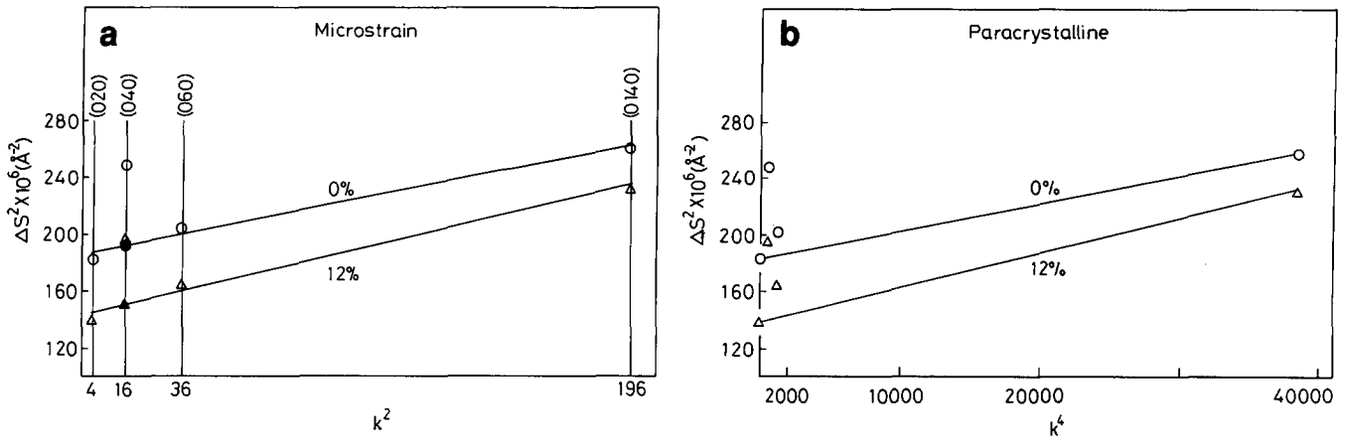

Figure 3 (a) Plot of ΔS^2 *versus* k^2; (b) plot of ΔS^2 *versus* k^4 (○, △ show experimental values and ●, ▲ represent calculated data for 0% and 12% stretched samples, respectively)

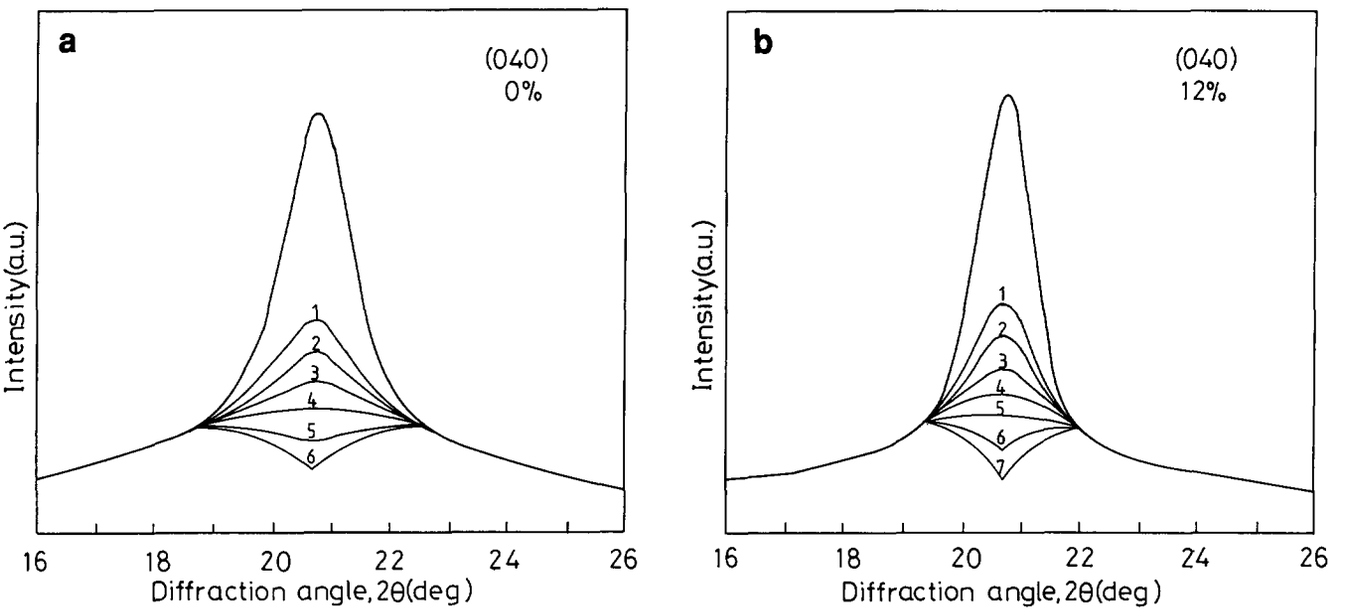

Figure 4 The meridional profiles of the amorphous scattering (number 1–7) evaluated from equation (5) by using different values of factor A for (a) 0% and (b) 12% stretched samples

does not lie on the line, but deviates significantly in both *Figures 3a* and *b*. The deviation of the (040) profile must be due to an inadequate evaluation of the amorphous scattering, which has a peak overlapping on the crystal (040) diffraction. The true meridional (040) profile should have the breadth due to the crystallite size and lattice disorder, and should lie on the line made by other (0*k*0) profiles in *Figure 3a*. This leads to the expectation that the true (040) profiles should have the integral breadth $2\Delta\theta$, which is 0.68 and 0.64 (by using equation (2) where $\cos\theta_{040}$ and $\cos\theta_{0140}$ are 0.984 and 0.779) times as narrow as that of each (0140) profile for 0% and 12% stretched samples, respectively. Under this expectation, the (0140) profile was redrawn so that the breadth might become 0.68 and 0.64 times as narrow, which was denoted by $I^{red}_{(040)}$. The true crystal (040) intensity, $I^{cr}_{(040)}$, is given by a product of $I^{red}_{(040)}$ with a numerical factor A, which is independent of scattering angle in the range of the (040) diffraction peak. Then the true amorphous scattering overlapping on the (040) diffraction, $I^{am}_{(040)}$, at a given scattering angle 2θ near the (040) diffraction, is given by

$$I^{am}_{(040)} = I^{obs}_{(040)} - AI^{red}_{(040)} \quad (5)$$

where $I^{obs}_{(040)}$ is the observed (040) intensity at a given 2θ. Thus if A is chosen appropriately, the profile of the amorphous scattering overlapping on the (040) diffraction can be estimated. As can be seen from these explanations, the originality of this method lies in the idea that the amorphous scattering peak is evaluated by using the crystal diffraction profile, but without assuming a priori the profile of the amorphous scattering.

Figures 4a and *b* show the calculated amorphous scattering profiles, $I^{am}_{(040)}$ in 0% and 12% stretched samples for different values of A from 0.7 to 1.3. It is clear that the profiles of numbers 5 and 6 (*Figure 4a*) and numbers 6 and 7 (*Figure 4b*) are meaningless, because the shapes of the profile are unreasonable for amorphous scattering, so these values of A could be avoided. However, it is still difficult to estimate the true profile of amorphous scattering and a difficulty remains in

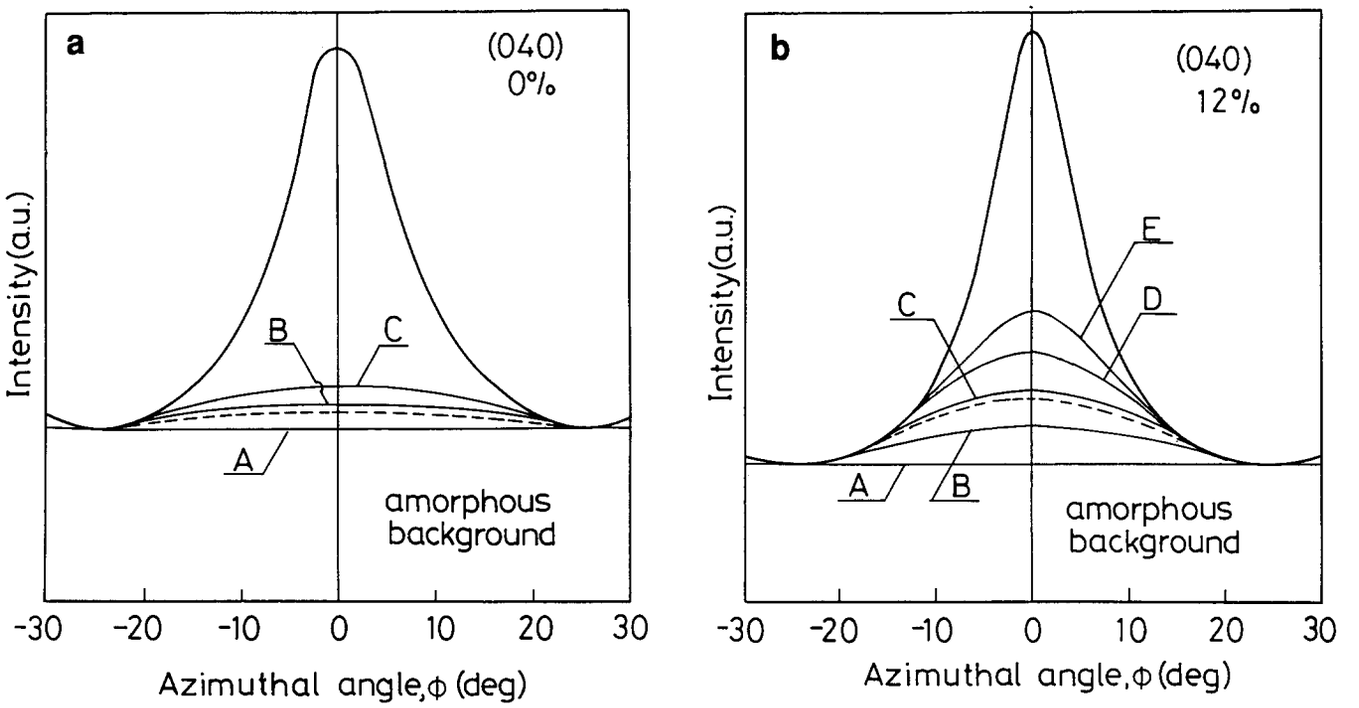

Figure 5 The azimuthal intensity profiles of (040) for (a) 0% and (b) 12% stretched samples: the solid lines A–E show the amorphous background for evaluating f_c and the broken lines represent the real azimuthal profile of calculated amorphous background

Table 1 The crystallite orientation function, f_c, evaluated from the (0*k*0) azimuthal profiles by using the amorphous background A–E in *Figure 5*

	f_c	
Stretch:	12%	0%
0140A	0.970	0.962
060A	0.972	0.964
040A	0.962	0.961
040B	0.966	0.964
040C	0.974	0.967
040D	0.980	
040E	0.986	

choosing a correct factor A. Consequently our interest is concentrated on determining this factor.

The crystallite orientation function, f_c, is given by

$$f_c = (3\langle\cos^2\phi\rangle - 1)/2 \quad (6)$$

$$\langle\cos^2\phi\rangle = \frac{\int_0^{\pi/2} I(\phi)\cos^2\phi\sin\phi\,d\phi}{\int_0^{\pi/2} I(\phi)\sin\phi\,d\phi} \quad (7)$$

where $\langle\cos^2\phi\rangle$ represents the mean-square cosine of the azimuthal angle ϕ of the chain axis corresponding to the fibre axis of a sample and $I(\phi)$ is the (0*k*0) azimuthal intensity distribution. The values of f_c estimated from any azimuthal distribution of the (0*k*0) intensities should be equal to each other independently of k, and if not, this would be mainly due to the error in the evaluation of amorphous scattering.

The values of f_c were first evaluated from the (0*k*0) azimuthal profile, by using the baseline A for the amorphous scattering in *Figure 5*, with the results shown in *Table 1*. It is noted that the values for f_c from the (060) and (0140) intensity distributions are nearly the same, while that from the (040) distribution is smaller. This indicates the error in the evaluation of the (040) azimuthal intensity distribution, which is due to an error in evaluating the amorphous scattering. The smaller value of f_c estimated from the (040) diffraction than from the others in *Table 1* implies that the intensity of the amorphous scattering has an azimuthal distribution that has the peak maximum at $\phi = 0°$, as shown in *Figure 5*, because of the high orientation. Since the real azimuthal amorphous intensity distribution is difficult to evaluate, it is assumed here that the distribution is given by a smooth curve such as B–E shown in *Figure 5*. These curves were drawn as smoothly as possible so that each of them might have a given peak height h and pass both ends of the azimuthal intensity profile (see *Figure 6*). The values of f_c were evaluated for each curve from background and compared with values from the (0140) and (060) diffractions, since when the value of h is correctly chosen, the value of f_c from the (040) should be equal to those from (060) and (0140).

Calculated results are shown in *Table 1*. It is noted that the increase in h monotonically increases the calculated value of f_c and that the real background curve may be between curves B and C for the 12% stretched sample, while for the 0% sample it is difficult to determine correctly, although it seems to be between A and B. The amorphous background of the (040) azimuthal profile was obtained by repeating this procedure and is shown by broken lines in *Figure 5*. It is noted that the true crystal (040) peak intensity at $\phi = 0°$ can be used to determine the factor A in equation (5). Because 2θ *versus* intensity ($I(2\theta)$) and ϕ *versus* intensity ($I(\phi)$) profiles for the (040) diffraction must have a relationship between each other, shown schematically in *Figure 6*, where O corresponds to $2\theta = 20.45°$ and $\phi = 0°$ commonly for both profiles, when $h(=\overline{PQ})$ has been obtained by the above procedure, and in other words, the point Q is

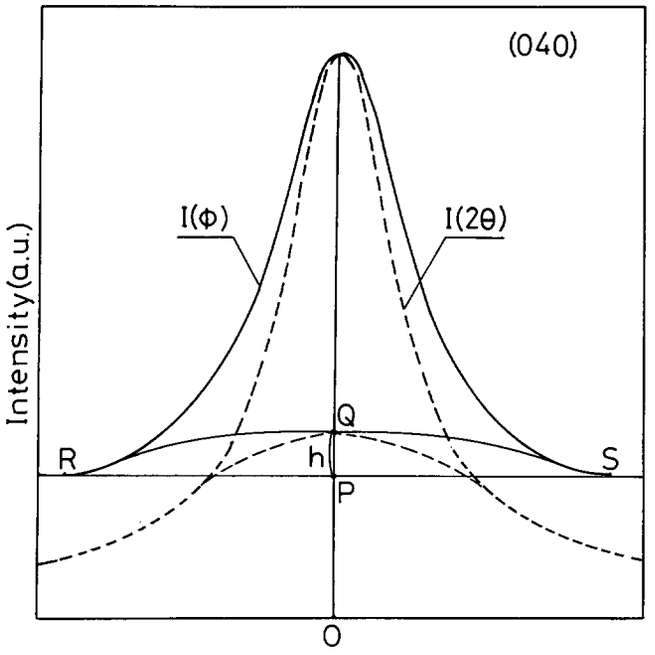

Figure 6 A schematic plot of the relation between 2θ *versus* intensity ($I(2\theta)$) and ϕ *versus* intensity ($I(\phi)$) profiles: curve RQS represents an estimated azimuthal profile of the amorphous background

fixed, it is possible to estimate the factor A in equation (5). The calculated values of the factor A are *ca.* 1.05 and 0.95 for 0% and 12% stretched samples, respectively. According to these procedures, it is possible to estimate the profile of the meridional amorphous scattering overlapping on the (040) diffraction from the data in *Figure 4*.

Figure 7 shows those meridional amorphous scattering profiles estimated for 0% and 12% stretched samples, which are obtained by using 1.05 and 0.95 for A, respectively. *Figure 7* indicates that the 12% stretched sample has a more concentrated amorphous scattering profile than the original one. This means that amorphous chains are more oriented along the fibre axis under extension. It should be noted the accuracy of the resulting amorphous scattering profiles is higher in the 12% stretched sample than in the original one.

All the results indicate that in the nylon-6 fibre the amorphous scattering concentrates on the meridian, particularly under extension. Roughly speaking, the amorphous scattering peak appearing at *ca.* $2\theta = 20.45°$ must be contributed by both inter- and intra-chain scatterings. It is well known that this peak appears in both semicrystalline and amorphous polymers[15–18]. In uniaxially oriented materials, the scattering due to inter-chain interference must tend to concentrate on the equator, while the intra-chain scattering must concentrate on the meridian[9,10]. The latter is the case of interest in this work. However, we have no other quantitative explanations for this meridional concentration of the amorphous scattering at $2\theta = 20.45°$. A cylindrical distribution function (CDF)[19,20] of the amorphous phase, which is obtained by Fourier transformation of the amorphous scattering in a wide range of 2θ and ϕ, is expected to give the best information about this problem. However, the difficulty in separating the amorphous scattering over a wide range of 2θ and ϕ has not been overcome.

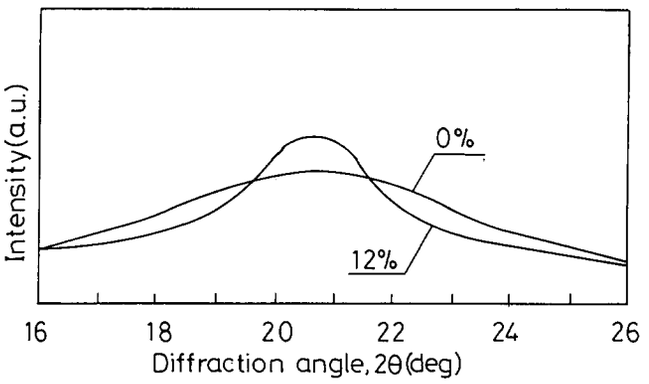

Figure 7 The calculated meridional profiles of the amorphous scattering for 0% and 12% stretched samples

CONCLUSIONS

A new method of evaluation for the meridional amorphous X-ray scattering of nylon-6 fibres is proposed in this study. This method can only be applied to samples that have a series of systematic crystal diffractions and a highly oriented structure. The results on nylon-6 fibres show that this method can be used to evaluate effectively meridional amorphous scattering. The reason for the concentration of scattering intensity has not yet been discovered, but at least this method presents a procedure for evaluating the amorphous scattering from semi-crystalline polymers and provides a scattering profile. The experimental results show that the change of observed (040) profile with extension is due not only to the increase of crystallite size, but also to the real concentration of the amorphous scattering.

REFERENCES

1 Kaji, K. *Makromol. Chem.* 1974, **175**, 311
2 Alexander, L. E. 'X-ray Diffraction Methods in Polymer Science', Wiley-Interscience, New York, 1969, p. 137
3 Polizzi, S., Fagherazzi, G., Benedetti, A., Battagliarin, M. and Asano, T. *Eur. Polym. J.* 1991, **17**, 85
4 Guerrero, S. J., Veloso, H. and Randon, E. *Polymer* 1990, **31**, 1615
5 Balta-Calleja, F. J. and Vonk, C. G. 'X-ray Scattering of Synthetic Polymers', Elsevier, New York, 1989, p. 175
6 Murthy, N. S. and Minor, H. *Polymer* 1990, **31**, 996
7 Heuvel, H. M. and Huisman, R. *J. Polym. Sci., Polym. Phys. Edn* 1981, **19**, 121
8 Gurato, G., Fichera, A., Grandi, F. Z., Zannetti, R. and Canal, P. *Makromol. Chem.* 1975, **175**, 953
9 Williams, J. L., Karam, H. J., Cleereman, K. J. and Rinn, H. W. *J. Polym. Sci.* 1952, **8**, 345
10 Pick, M., Lovell, R. and Windle, A. H. *Polymer* 1980, **21**, 1017
11 Holmes, D. R., Bunn, C. W. and Smith, D. J. *J. Polym. Sci.* 1955, **17**, 159
12 Hosemann, R. and Bagchi, S. N. 'Direct Analysis of Diffraction by Matter', North-Holland, Amsterdam, 1962
13 Warren, B. E. *Prog. Met. Phys.* 1959, **8**, 147
14 Murthy, N. S. *J. Polym. Sci., Polym. Phys. Edn* 1986, **24**, 549
15 Kakudo, M. and Ulman, R. *J. Polym. Sci.* 1960, **45**, 91
16 Sakurada, I., Nukushina, Y. and Mori, N. *Kobunshi Kagaku* 1955, **12**, 302
17 Krimm, S. and Tobolsky, A. V. *Textile Res. J.* 1951, **21**, 805
18 Ohno, R., Miyasaka, K. and Ishikawa, K. *Kobunshi Kagaku* 1972, **29**, 327
19 Norman, N. *Acta Crystallogr.* 1965, **7**, 462
20 Mitchell, G. R. and Lovell, R. *Acta Crystallogr.* 1981, **A37**, 189